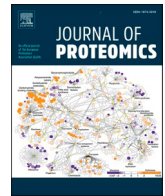




Since January 2020 Elsevier has created a COVID-19 resource centre with free information in English and Mandarin on the novel coronavirus COVID-19. The COVID-19 resource centre is hosted on Elsevier Connect, the company's public news and information website.

Elsevier hereby grants permission to make all its COVID-19-related research that is available on the COVID-19 resource centre - including this research content - immediately available in PubMed Central and other publicly funded repositories, such as the WHO COVID database with rights for unrestricted research re-use and analyses in any form or by any means with acknowledgement of the original source. These permissions are granted for free by Elsevier for as long as the COVID-19 resource centre remains active.



Membrane proteomic analysis identifies the polarity protein PARD3 as a novel antiviral protein against PEDV infection

Huimin Huang^a, Yongtao Li^a, Li Wang^b, Yapeng Song^a, Gaiping Zhang^{a,b,c,*}

^a College of Veterinary Medicine, Henan Agricultural University, Zhengzhou 450002, China

^b Key Laboratory of Animal Immunology of the Ministry of Agriculture, Henan Provincial Key Laboratory of Animal Immunology, Henan Academy of Agricultural Sciences, Huayuan Road No. 116, Zhengzhou 450002, China

^c Jiangsu Co-innovation Center for Prevention and Control of Important Animal Infectious Diseases and Zoonoses, Yangzhou 225009, China

ARTICLE INFO

Keywords:

Membrane proteomic
PEDV
PARD3
Tight junction
Cell polarity
PDZ domain

ABSTRACT

Porcine epidemic diarrhea virus (PEDV) is a highly pathogenic enteric coronavirus causing lethal watery diarrhea in suckling piglets. PEDV could remodel host membrane structures for their replication, assembly and escape from host cells. However, little is known about the host membrane proteins of PEDV infection. In this study, we analyzed differentially abundant proteins (DAPs) between PEDV infection group and control group and identified the polarity protein PARD3 as one of the most significantly DAPs. PARD3 is implicated in the formation of tight junctions at epithelial cell-cell contacts. Then, we found that PEDV infection promoted the degradation of PARD3 via the ubiquitin proteasome pathway. Moreover, knockdown of PARD3 promoted the proliferation of PEDV. Further study showed that the downregulation of PARD3 altered the normal morphology of the tight junction proteins and promoted apical and basolateral virus proliferation. Tight junctions enable epithelial cells to form physical barriers, which act as an innate immune mechanism that can impede viral infection and PEDV affected the barrier functions by causing degradation of PARD3. Taken together, this work is the first time to investigate the membrane protein profile of PEDV-infected cells using quantitative proteomics and suggests that PARD3 could be a potential novel antiviral protein against PEDV infection.

Significance: Membrane proteins are involved in various physiological and biochemical functions critical for cellular function. It is also dynamic in nature, where many proteins are changed during in response to environmental stress. However, membrane proteins are difficult to study because of their hydrophobicity. Membrane proteomic methods using mass spectrometry analysis have been developed and applied for the characterization of the plasma membrane and subcellular organelles of various virus infected cells. Porcine epidemic diarrhea virus (PEDV) is an enteric pathogen of importance to the swine industry, causing high mortality in neonatal piglets. Because PEDV infected Vero cells can lead to significant changes in cell membrane morphology and form syncytial lesions. Here, we isolated the membrane proteins of PEDV infected and control cells and applied isobaric tags for relative and absolute quantification (iTRAQ) labeling coupled with liquid chromatography-tandem mass spectrometry (LC-MS/MS) to quantitatively identify the differentially abundant proteins (DAPs) in PEDV-infected Vero cells and confirmed the DAPs by performing RT-qPCR and Western blot analysis. Among these differential proteins, we focused on a down-regulated protein PARD3 which is important for cell tight junction and cell polarity. Loss of PARD3 can destroy the tight junction of cells and promote the proliferation of PEDV in the apical and basolateral sides. These findings will provide valuable information to better understand the mechanisms underlying the host defense responses to PEDV infection.

1. Introduction

Coronaviruses (CoVs) constitute a family of enveloped viruses with single-stranded positive-sense RNA genomes, which pose a threat to the

health of various mammals and birds [1]. Porcine epidemic diarrhea virus (PEDV) is an etiological agent of porcine epidemic diarrhea and belongs to the genus Alphacoronavirus in the family Coronaviridae [2]. PEDV infection is characterized by watery diarrhea, vomiting and

* Corresponding author at: College of Veterinary Medicine, Henan Agricultural University, Zhengzhou 450002, China.

E-mail address: zhanggaip@126.com (G. Zhang).

<https://doi.org/10.1016/j.jprot.2021.104462>

Received 1 September 2021; Received in revised form 1 December 2021; Accepted 17 December 2021

Available online 23 December 2021

1874-3919/© 2021 Elsevier B.V. All rights reserved.

dehydration [3]. The virus has caused significant economic and public health concerns since its discovery in the late 1970s and now occurs worldwide in most major swine-raising countries [4]. Enveloped virus particles introduce their genetic materials into organisms by binding to cell receptors and then fusing with viral and cell membranes. The PEDV spike protein (S) is a class I viral membrane fusion protein and is the key protein responsible for virus entry into target cells [5]. S protein can be cleaved into two domains by proteases with distinct functions: the N-terminal S1 subunit responsible for receptor binding and C-terminal membrane anchored S2 domain responsible for membrane fusion [5,6]. Some endogenous proteases in the small intestines of pigs may promote the entry of the PEDV into intestinal epithelial cells. However, in vitro, PEDV-infected cells produce syncytia only after treatment with an exogenous protease and greatly promote the proliferation of the virus. These features are similar to those of other CoVs, such as severe acute respiratory syndrome coronavirus (SARS-CoV), SARS-CoV-2 and mouse hepatitis virus (MHV) [7–9].

PEDV enters host cells through intricate interactions with cell membrane proteins and lipids, and utilize microfilamentous proteins as tracks or move them when they break through membrane barriers [10]. Intercellular tight junctions (TJs) form a physical fence which protects underlying tissues from pathogen invasion and define epithelial apico-basal polarity [11]. Three kinds of TJ proteins: Zonula occludens (ZO), Occludin and Claudins, are essential to the maintenance of epithelial barrier integrity and permeability [12]. Some viruses can destroy TJs and hijack the different components of TJs to initiate their infection. The SARS-CoV E protein can alter TJ formation, affects polarity and modifies the subcellular distribution of PALS1, a tight junction-associated protein [13]. The Coxsackie virus disrupts TJ assembly by decreasing Claudin-4, E-cadherin and ZO-1 levels, infects epithelial cells and spreads to neighboring cells [14]. Influenza viruses (H1N1 and H5N1) can induce epithelial cell barrier disruption, significantly decrease trans-barrier electrical resistance (TER) level and increase permeability [15]. As important parts of the intestinal mucosal barrier, TJs are integral to the maintenance of the mechanical barrier and permeability of the intestinal mucosal epithelium [16]. Epithelial cell integrity is essential to the prevention of viral infections. TGEV and PEDV can impair the barrier integrity of cells by downregulating some proteins of tight and adherent junctions [17,18]. However, it remains largely unclear how PEDV breaks through the host cell barriers.

Although there have been proteomics on PEDV, including various strains and cells [19–22]. However, none of the prior studies included a global assessment of membrane proteins related to PEDV infection. Under the action of exogenous protease, the cell membrane of Vero cells infected with PEDV rearranged and formed typical syncytial lesions. We hypothesized that the changes in membrane protein abundance may reveal its mechanism. Herein, we profiled membrane proteins changes between PEDV-infected Vero cells and control group combined with quantitative iTRAQ LC-MS/MS Proteomics analysis. We also showed that polarity protein PARD3 was significantly downregulated in PEDV infection group which might be contributed to the destruction of tight junctions of cells by viruses. In general, these findings will contribute to a better understanding of the role of membrane proteins in PEDV infection and demonstrate PARD3 is a novel antiviral protein against PEDV infection.

2. Materials and methods

2.1. Cells and viruses

Vero cell (an African green monkey kidney cell line) was obtained from National Collection of Authenticated Cell Cultures and cultured in Dulbecco's Modified Eagle Medium (DMEM) supplemented with 10% FBS. IPEC-J2 cells (a porcine small intestinal epithelial cell line) are derived from experimental preservation and cultured in DMEM/F12 medium containing 10% FBS. The PEDV wildtype strain (HNXX) used in

this study was successfully isolated in our laboratory (Accession no. MK124712) and can form syncytial lesions with 3 µg/mL trypsin (Sigma T8802), and the reproductive cycle is 8 h. The cell-adapted strain of DR13 with green fluorescent protein (DR13-GFP) (doi:<https://doi.org/10.1371/journal.pone.0069997>) was a gift from Professor Wengtao Li and was propagated according to the method in the article. The DR13-GFP strain is constructed by PEDV-DR13 (GB:JQ023162) with the GFP gene added to the S gene and recombined as rPEDV-SDR13-GFP, and its proliferation does not require trypsin and the reproductive cycle is 7 h.

2.2. Extraction of membrane proteins of Vero cells

Vero cells were covered with a monolayer and washed twice with serum-free medium in 10 cm cell culture dishes. Then, the cells were infected with PEDV strain HNXX at a multiplicity of infection (MOI) of 0.1 and incubated with serum-free DMEM containing 3 µg/mL trypsin. The PEDV-infected or control uninfected cells were collected at 18 h postinfection (p.i.). Infected and mock groups were collected as biological replicates from three independent experiments. Extract the membrane protein according to the operation instructions of the natural membrane protein extraction kit (Merck 444,810).

2.3. Protein preparation, digestion, and labeling with iTRAQ labeling

Protein concentration was determined using the Pierce™ BCA Protein Assay Kit (Thermo) and confirmed by SDS-PAGE. We digested 100 µg of each sample at 37 °C for 12 h with sequencing grade modified trypsin (Promega, Madison, WI, USA). iTRAQ labeling was performed according to the manufacturer's instructions (AB SCIEX, iTRAQ 8PLEX, Lot number:A8029). Protein samples from the control group were labeled with tags 113, 114, and 117, while those from the PEDV-infected group received tags 118, 119, and 121 (three replicates/group). The labeled samples were then mixed and dried by vacuum centrifugation.

2.4. LC-MS/MS analysis of the membrane proteome

The equal amounts of polypeptide samples were redissolved by UPLC loading buffer and separated by reversed-phase C18 column (ACQUITY UPLC BEH C18 Column 1.7 µm, 2.1 mm × 150 mm Waters, USA) with high pH. According to the peak type and time, 20 fractions were collected and combined into 10 fractions. After vacuum centrifugation and concentration (rotation vacuum concentration, Christ RVC 2-25, Christ, Germany), the fractions were dissolved in mass spectrometry loading buffer and analyzed by two-dimensional liquid chromatography tandem mass spectrometry. MS was performed with scan range (M/z) 350–1300, acquisition mode DDA, Top 20 (select the 20 with the strongest signal among the parent ions for secondary fragmentation); The resolution of the first-order mass spectrum was set to 70,000, the fragmentation mode was set for HCD, the second-order resolution was 17,500, and the dynamic exclusion time was set to 18 s.

2.5. RNA extraction and real-time PCR

The total RNA was extracted from cells with TRIzol reagent (Invitrogen) according to the manufacturer's instructions. First-strand cDNA was synthesized by using PrimeScript RT Master Mix (Takara). Real-time PCR (RT-PCR) with probe method was used to determine the copy number of PEDV [23]. The relative expression level of each target gene was calculated by normalizing for GAPDH levels using the Comparative Ct Method ($\Delta\Delta Ct$ Method), and presented relative to the control sample. The primer sequences used in this paper are in the supplementary materials.

2.6. Western blotting

Cells were washed with phosphate buffer saline (PBS) and lysed in

ice-cold lysis buffer (RIPA lysis buffer, Beyotime) with protease inhibitor cocktail (Beyotime). Protein concentration was determined with a Pierce BCA Protein Assay Kit (Thermo). Samples containing equal amounts of protein were separated SDS-PAGE and transferred to a PVDF membrane. The membrane was blocked with 5% nonfat milk in PBS containing 0.1% Tween 20 (PBST), then incubated overnight at 4 °C with primary antibodies, then rinsed and incubated with the corresponding HRP-conjugated secondary antibodies for 60 min then detected by autoradiography using ECL. Western blotting was quantified by Gel & chemiluminescence imaging system (Vilber France). The intensity of the bands in terms of density was measured and normalized against GAPDH. All data were presented as means \pm SD of three independent. The specific information of the antibodies used in this study is in the supplementary materials.

2.7. Indirect immunofluorescence assay

Vero cells cultured in Glass Bottom Culture Dishes (NEST) covered in a monolayer and washed with PBS for 3 times and inoculated with PEDV. The cells were rinsed with PBS after infection and then fixed with 4% paraformaldehyde under room temperature (RT) for 15 min, permeabilized with 0.1% Triton X-100 for 5 min, blocked with 1% bovine serum albumin (BSA) under RT for 1 h, and then stained with Primary antibody at 4 °C overnight. Then the cells were incubated with the secondary antibody under RT for 1 h. Between each step, the cells were washed five times with PBST. The immunofluorescence images were taken with a laser scanning confocal microscopy (Zeiss LSM 800).

2.8. Small interfering RNA transfection

Vero cells were grown to approximately 80% confluence and then transiently transfected with small interfering RNA (siRNA) according to the operation steps of RNAiMAX (Invitrogen). The siRNA sequences are as follows: PARD3-460: 5'-3'GGAUACAAGUGCAUCGCUUTT; PARD3-2352: 5'-3'GCUGCUCUCAGUAGGAUAATT; PARD3-3521: 5'-3'GCGUCUGAGGCAAGAAUUUTT. A scrambled siRNA was used as a negative control. The silencing efficiency was determined by Western blot after transfection for 36 h.

2.9. Infection of PEDV on Transwell

Transwell (pore size 8 μ m, Costar) that polycarbonate membrane filters attached to the bottom of plastic cups were placed into 24-well tissue culture plates. Subsequently, 200 μ L of cell suspension containing 5×10^4 cells were added to each filter, while 600 μ L/well of cell growth medium was added to each well of the 24-well plate. When the cells adhered and grew to 80%, siRNA was transfected. After 36 h the tightness of the monolayers was checked by adding DMEM containing phenol red to the low chambers and without phenol red in the upper chamber. Filter-grown Vero cells were infected with PEDV-DR13-GFP (MOI = 0.1) from either upper chamber or low chambers after the cells had become highly polarized as determined the tightness of monolayers. Infection was allowed to take place for 1 h at 37 °C, after which the inoculum was removed. The filter-grown cells were washed with PBS and culture medium was added. The quantity of virus infected cells is determined by the number of lesions formed by virus on cells.

2.10. Adsorption and internalization of PEDV

The cells were pre-chilled for 10 min and inoculated with PEDV (MOI = 1) at 4 °C for 1 h for virus binding. Then the cells were washed five times with ice-cold PBS to remove unbound viruses, collect cells from this step to determine the adsorption of virus. After the virus was adsorbed at 4 °C, washed five times with ice-cold PBS to remove unbound viruses, then immediately warmed to 37 °C to initiate internalization. After incubation 60 min, the cells were treated with

proteainase K (0.5 mg/mL) at 4 °C for 30 min and then washed with PBS to inactivate and remove the non-internalized PEDV particles. The cells were collected and subjected to RT-PCR analysis.

2.11. Drug treatments

Vero cells were treated with the proteasome inhibitor MG132 (5 μ M; Beyotime) and the autophagy inhibitor 3-Methyladenine (3-MA) (5 mM; Solarbio), the carrier control dimethylsulfoxide (DMSO) for 1 h before they were inoculated with a mock infection control or PEDV. Cells were further cultured in the presence of MG132, 3-MA, or DMSO for the indicated times. Then the cells were collected and analyzed by Western blotting.

2.12. Extraction of subcellular components

The Vero cells subcellular components were extracted at 18 h p.i. from PEDV (HNXX) infected group and control group according to the Membrane, Nuclear and Cytoplasmic Protein Extraction kit (Sangon Biotech NO. C510002). The changes of PARD3 were detected by Western blotting and GAPDH is the internal reference of cytoplasmic protein and Histone H3 corresponding to nuclear protein.

2.13. Statistics

For data analysis, protein quantification data with $p < 0.05$ & (FC < 0.83 or FC > 1.20) was selected as the DAPs.

The experiments in this paper were performed with three independent experiments, and the calculated results were presented as mean \pm standard deviation (SD). Statistical analyses were performed using student's t-test. Graph Pad Prism5.0 was used to analyze the statistics in this study. The statistical significances were defined as $p < 0.05$ (*), and the higher significance was denoted by $p < 0.01$ (**) and $p < 0.001$ (***)

3. Results

3.1. Identification and analysis of membrane proteins in PEDV-infected Vero cells

To determine the kinetics of PEDV propagation in Vero cells, viral titers were calculated as TCID₅₀ units on basis of the viral-induced cytopathic effect (CPE) at 6, 12, 18, 24, 30 and 36 h p.i.. As shown in Fig. 1A, some cells fused and lost their individual demarcation at 18 h p.i., and obvious CPE were observed at 24 and 30 h p.i.. Numerous distinctly swollen nuclei accumulated in the centres of the rounded polycarions. The titer of the virus started to increase at 6 h, peaked at 30 h, and then decreased (Fig. 1B). To capture the intact cell membrane at the same time as the occurrence of lesions caused by PEDV, membrane proteins were collected at 18 h p.i.. Western blot analysis was used to confirm the extracted membrane proteins (Fig. 1C). Quantitative membrane proteomics were used in analyzing host DAPs in PEDV-infected Vero cells and the control group. In this quantitative proteomics experiments results, a total of 4579 proteins were identified (in the Supplementary materials 2). Significantly upregulated or down-regulated proteins were determined with a p -value of < 0.05 and FC of < 0.83 or > 1.20 . After bioinformatics data analysis, ten proteins were found significantly upregulated, and eleven proteins were markedly downregulated after virus infection. Approximately 47% of these proteins were membrane proteins or membrane-associated proteins. The remaining proteins were predicted to localize to the cytoplasm, mitochondria and nuclei, and some of them were detected previously in the other membrane proteome studies (in the Supplementary materials Table1 and Fig. 1D). The mass spectrometry proteomics data have been deposited to the ProteomeXchange Consortium (<http://proteomecentral.proteomexchange.org>) via the iProX partner repository [24] with

the dataset identifier PXD029763.

To confirm PEDV-induced changes in protein abundance, five proteins were subjected to Western blot analysis with specific antibodies, and 10 proteins were analyzed by RT-PCR assays. The proteins were selected on the basis of interest and different ratios. Although the verified proteins were relatively limited, the results of Western blot analysis were basically in line with those obtained with membrane proteomics (Fig. 1E). However, the mRNA levels of PARD3, AIDA and METTL17 in the PEDV-infected cells showed no significant changes (Fig. 1F), indicating that the downregulation was due to post-transcriptional events.

3.2. Changes in PARD3 after PEDV infection

To closely monitor the content of PARD3 in PEDV-infected cells, we examined 2, 4, 6, 8, 10 and 12 h p.i. by Western blotting. As expected, PARD3 was significantly downregulated at 6 h p.i. (Fig. 2A). With the virus infection, the content of PARD3 decreased significantly. The DR13 strain which requires neither trypsin nor syncytial lesions during

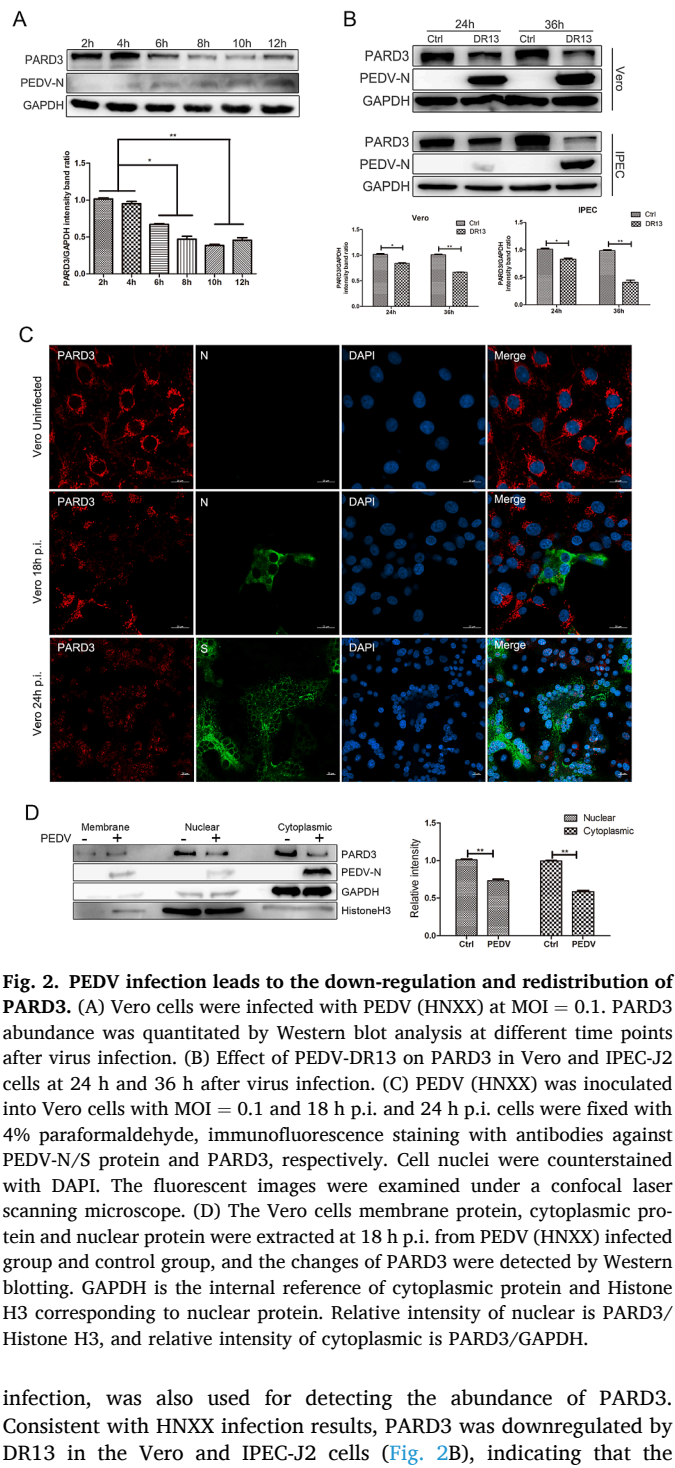


Fig. 2. PEDV infection leads to the down-regulation and redistribution of PARD3. (A) Vero cells were infected with PEDV (HNXX) at MOI = 0.1. PARD3 abundance was quantitated by Western blot analysis at different time points after virus infection. (B) Effect of PEDV-DR13 on PARD3 in Vero and IPEC-J2 cells at 24 h and 36 h after virus infection. (C) PEDV (HNXX) was inoculated into Vero cells with MOI = 0.1 and 18 h p.i. and 24 h p.i. cells were fixed with 4% paraformaldehyde, immunofluorescence staining with antibodies against PEDV-N/S protein and PARD3, respectively. Cell nuclei were counterstained with DAPI. The fluorescent images were examined under a confocal laser scanning microscope. (D) The Vero cells membrane protein, cytoplasmic protein and nuclear protein were extracted at 18 h p.i. from PEDV (HNXX) infected group and control group, and the changes of PARD3 were detected by Western blotting. GAPDH is the internal reference of cytoplasmic protein and Histone H3 corresponding to nuclear protein. Relative intensity of nuclear is PARD3/Histone H3, and relative intensity of cytoplasmic is PARD3/GAPDH.

infection, was also used for detecting the abundance of PARD3. Consistent with HNXX infection results, PARD3 was downregulated by DR13 in the Vero and IPEC-J2 cells (Fig. 2B), indicating that the downregulation of PARD3 was caused by PEDV infection regardless of whether syncytial lesions formed or not. We also infected IPEC-J2 with PEDV (HNXX), but its proliferation on IPEC-J2 cells was not obvious. Hence, the downregulation of PARD3 was not significant (data not shown).

Concurrently, PARD3 abundance was evaluated through IFA using anti-PARD3 antibody at 18 and 24 h p.i. (Fig. 2C). Owing to the high level of PEDV-N protein at 24 h p.i., its distribution in the Vero cells was extremely wide, and the IFA signal was extremely strong for observation. Thus, we utilized an anti-S antibody. PARD3 cytoplasmic localization was significantly decreased at 18 h p.i., and nuclear aggregated obviously at the late period of infection when the large vacuoles were formed, the cytoplasm began to burst in the centers of syncytia and the

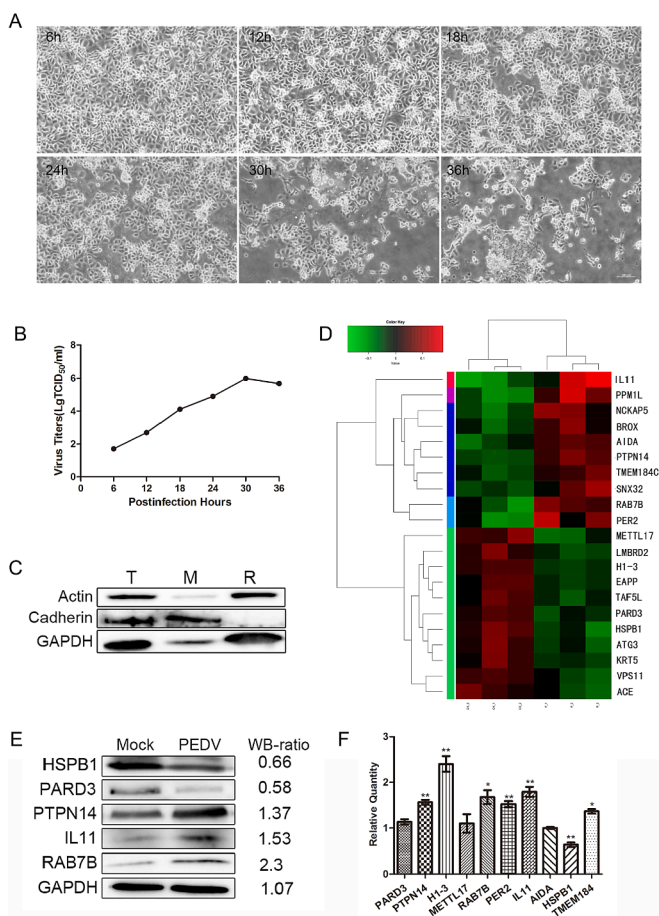


Fig. 1. Membrane proteomics of PEDV infected Vero cells. (A) The cytopathic effects (CPE) of Vero cells at 6, 12, 18, 24, 30, and 36 h after PEDV (HNXX) infection. (B) Growth curve of PEDV (HNXX) strain in Vero cells. (C) Verify the membrane protein extracted from Vero cells. Total lysate (T), Membrane fraction (M) and Remaining 'non-membranous' proteins (R). Cadherin and GAPDH were the membrane and non-membrane fractions markers respectively. An equal amount of protein from each sample was used for the Western blot analysis. (D) Heat-maps of differentially abundant proteins. (E) Analysis total protein of HSPB1, PARD3, PTPN14, IL11 and RAB7B in PEDV (HNXX)-infected and control samples. Infection/control ratios are shown on the right side. (F) RT-PCR analysis of the DAPs in infected cells and control. GAPDH served as a control. The multiple of changes relative to the control group was indicated by $p < 0.05$ (*), and the higher significance was denoted by $p < 0.01$ (**) and $p < 0.001$ (***)

nuclei became pycnotic. The distribution of PARD3 on the cell membrane was difficult to observe in the virus infection group compared that in the control group. The results showed that PEDV significantly reduced the abundance of PARD3 compared with the control and changed the location of PARD3. Moreover, we compared PARD3 abundance in different subcellular fractions in PEDV-infected and control cells. The Vero cells were inoculated with the PEDV for 18 h, and protein extracts were separated into membrane, nuclear and cytoskeletal fractions. The abundance of PARD3 was ascertained through Western blotting. Fig. 2D showed that PARD3 levels were obviously reduced in the cytoplasmic and nuclear fractions of the virus infection cells compared with the control cells. However, the changes of PARD3 in the cell membrane were not as obvious as the changes in the cytoplasm and nucleus. This

experiment, together with the results present above, indicate that PEDV induce the downregulation of PARD3 and change intracellular localization.

3.3. PEDV causes PARD3 degradation through the proteasome-dependent pathway

The downregulation of PARD3 by PEDV infection could be caused by incoming virions or by viral replication products. To test whether viral replication is needed for the interference effect, we inactivated PEDV virions by UV illumination and verified the inactivation by IFA and Western blotting after inoculation of Vero cells (Fig. 3A). When the UV-inactivated virus was used to inoculate Vero cells, PARD3 abundance

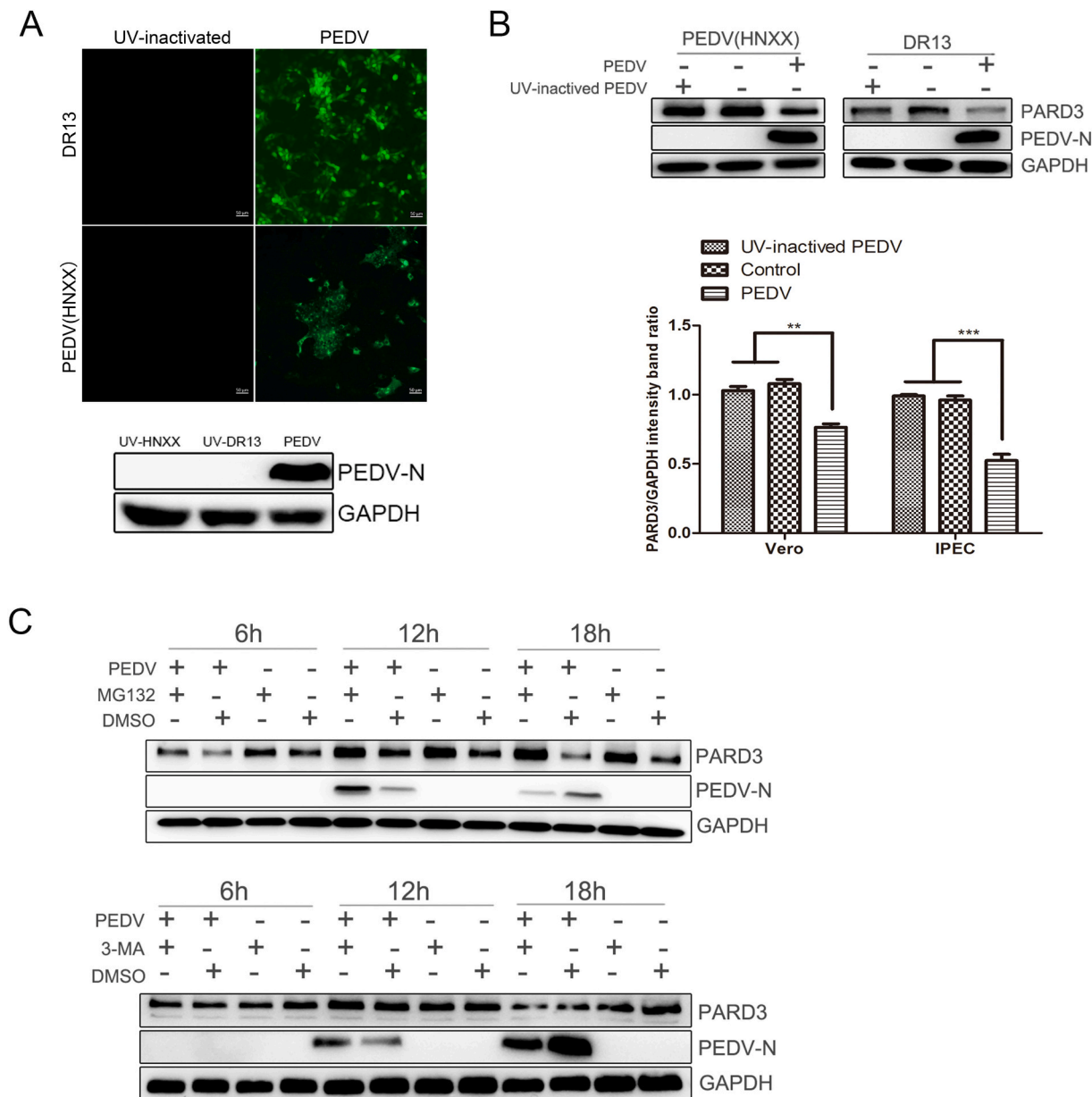


Fig. 3. PEDV induces PARD3 degradation through the proteasome-dependent pathway. (A) IFA and Western blot assay verified UV-inactivated PEDV was replication defective. UV-inactivated PEDV and live PEDV at a MOI of 0.1 infected Vero cells for 24 h. Cells were analyzed by IFA and Western blotting with a MAb against PEDV N protein. (B) The levels of PARD3 protein were not reduced by UV-inactivated PEDV in cells. Vero cells were inoculated with UV-inactivated PEDV at a MOI of 0.1 for 24 h while live PEDV using as a control. Western blotting was used to detect the levels of PARD3 protein. (C) Vero cells were first treated with proteasome inhibitor MG132 (5 μM) or autophagy inhibitor 3-MA (5 mM) or the carrier control DMSO for 2 h and then either infected with PEDV (HNXX) at a MOI of 0.1 or left uninfected. Cells were further cultured in the absence or presence of MG132/3-MA for various times as indicated. Cell lysates were collected and were subjected to Western blot analysis.

was similar to those in mock-inoculated cells (Fig. 3B). Similar results were observed in DR13. These results indicated that active PEDV replication was needed for the downregulation of PARD3.

Intracellular protein degradation has two main mechanisms: the ubiquitin–proteasome system (UPS) and the autophagy-lysosome pathway (ALP) [25]. Ubiquitination is a proteasomal degradation pathway has high selectivity, and the proteasome generally recognizes ubiquitinated substrates. Autophagy is a major lysosome-mediated intracellular degradation pathway [26]. Therefore, to determine the mechanism by which PEDV induces PARD3 degradation, the content of PARD3 protein was examined in cells treated with protease inhibitor, MG132 and 3-MA, which is commonly used to inhibit autophagy [27]. As shown in Fig. 3C, treatment with MG132 can block PARD3 degradation in PEDV-infected Vero cells at 6 h p.i. in the early stage of infection. However, 3-MA treatment cannot reverse PARD3 degradation at 18 h p.i. These data indicate that the degradation of PARD3 requires the replication of PEDV and is degraded through the UPS.

3.4. Knock-down of PARD3 promotes PEDV proliferation in Vero cells

To study the role of PARD3 in PEDV infection, we designed three siRNAs targeting PARD3. P-2352 was the most efficient one and thus used in further experiments (Fig. 4A). After PARD3 silencing, the virus invaded the surrounding cells quickly, and lesion duration was shortened. The formation of syncytia and the release of virus were faster than those in the control (Fig. 4B). The TCID₅₀ results showed that the PARD3-downregulated group produced more viruses than the control group (Fig. 4C).

In view of the down-regulation of PARD3 can promote the proliferation of PEDV. We wanted to know whether PARD3 affects the early stages of viral infection. Therefore, the effect of downregulation of PARD3 on virus adsorption and internalization were also determined. As expected, downregulation of PARD3 promoted the adsorption and internalization of PEDV in Vero cells (Fig. 4D). These data indicate that inhibition of PARD3 has a significant impact on the proliferation of PEDV by affecting the entry stage of virus infection.

3.5. Knockdown of PARD3 disrupts the tight junctions of Vero cells

Given that PARD3 is one of the key factors of TJs, we wanted to know how PEDV influence the formation of such intercellular junctions. The abundance and localization of ZO-1 and Occludin were analyzed by fluorescence microscope, which is a reliable marker for TJ assembly [28]. First, we studied the effect of PEDV on the TJs of Vero cells. In the control cells, Occludin (green) co-localised with ZO-1 (red) to form a continuous and smooth junctional structure of even thickness. Two hours p.i., Occludin and ZO-1 began to have breaks. With the virus infection, the performance was more obvious at 3 and 5 h p.i., and the TJs became discontinuous. The levels of ZO-1 and Occludin were detected through Western Blotting. With the virus infection, ZO-1 and Occludin were decreased clearly (Fig. 5A&5B). The results were consistent with previous results that TJ protein abundance decreased after PEDV infection [17,18]. Then we detected changes in ZO-1 and Occludin after PARD3 silencing. The cells were transfected with si-PARD3 for 36 h, ZO-1 and Occludin showed complex arrangements, and the distribution of proteins was spotty and intermittent (Fig. 5C). The distribution was not uniform, similar to that of structures in immature cell-cell contacts [29]. However, the suppression of PARD3 was efficient and specific and had no effect on ZO-1 and Occludin protein levels (Fig. 5D). The possible reason is that the downregulation of PARD3 affects the distribution of TJs but could not affect the content of ZO-1 and Occludin. These results show that downregulation of PARD3 disrupts tight junction assembly of Vero cells.

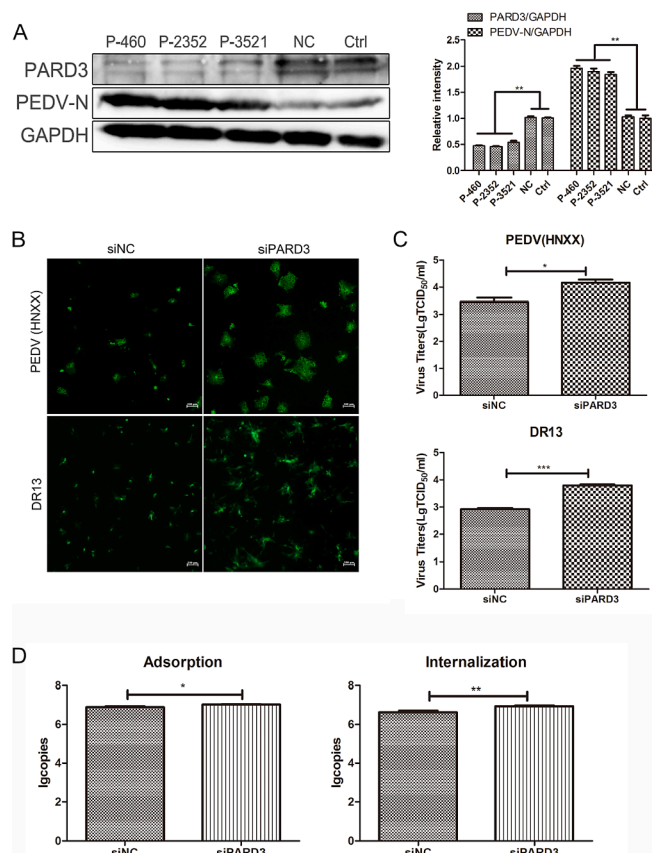


Fig. 4. Knockdown of PARD3 promotes PEDV proliferation. (A) Western blot detect the efficiency of the specific siRNAs. Three siRNA targeting PARD3, P-460 P-2352 and P-3521 and nontargeting control (NC) were transfected into Vero cells. Thirty-six hours after transfection, total proteins were analyzed. GAPDH served as a control. (B) IFA to detect PEDV infection in PARD3-deficient cells. After 36 h of transfection of Vero cells with siNC or siPARD3, the cells were infected with PEDV (HNXX) and DR13 with MOI = 0.1 and examined for PEDV infection at 24 h by IFA. (C) Determination of virus titer by TCID₅₀. Vero cells were treated with siRNA and virus infection as mentioned above. At 24 h p.i., the virus titer was determined by TCID₅₀ assay. (D) The effect of down-regulation of PARD3 on virus adsorption and internalization. 36 h after transfection of siPARD3 or siNC, the cells were infected with PEDV (HNXX) (MOI = 1). After the virus was absorbed and internalized, RNA was extracted from cells and PEDV content was detected by RT-PCR.

3.6. Knockdown of PARD3 promotes PEDV infection in the apical and basolateral sides

PARD3 polarizes a wide variety of animal cells, including epithelial cells, and is required for apico-basal epithelial polarity [30]. Epithelial cells grow with a polarized topology and are involved in the separation of the plasma membrane into apical and basolateral domains. The entry and release of some coronaviruses in polarized epithelial cells are restricted at the apical side and others enter and exit at both sites of polarized epithelial cells [31–34]. To investigate whether down-regulation of PARD3 affects PEDV infection in Vero cells through the apical or basolateral surface, we inoculated the cells on Transwell and transfected with siRNA-PARD3. To eliminate the effect of trypsin on cell morphology, the DR13 strain with GFP tag was used. After cells formed polarized monolayers, DR13-GFP was exposed on the apical or basolateral surface. These results illustrated that PEDV infection was significantly higher on the apical surface than on the basolateral surface (Fig. 6), which is consistent with the previous results [35]. PEDV on the basolateral side showed more infections in the PARD3-deficient cells. Depletion of PARD3 may abolish the functional integrity of TJs between

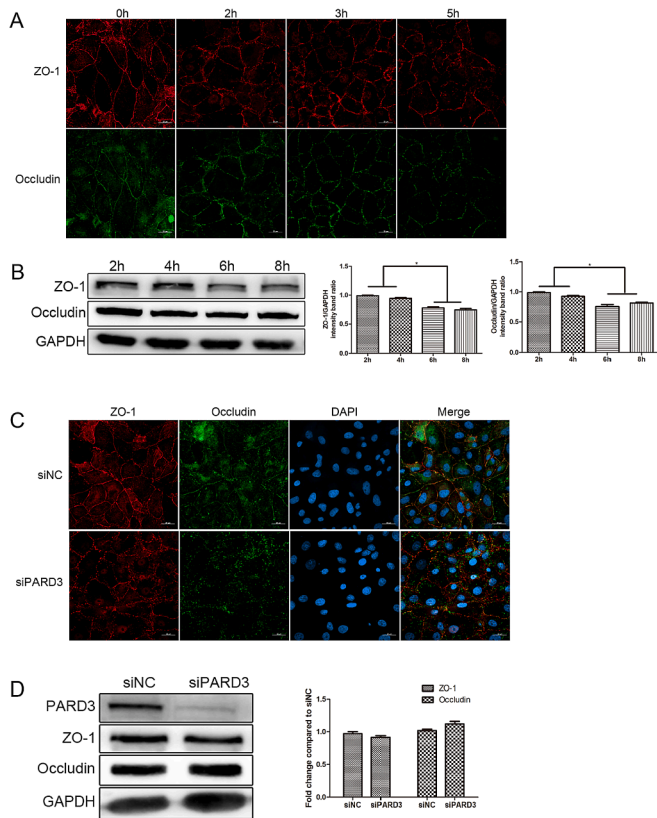


Fig. 5. Downregulation of PARD3 disrupts the tight junctions of Vero cells. (A–B) Patterns of ZO-1 and Occludin at different time points after PEDV infection. Vero cells were inoculated PEDV (HNXX) at MOI = 0.1 and collected at different time points after infection for IFA and Western blot. (C–D) Immunofluorescence was used to observe the effect of down regulated of PARD3 on ZO-1 and Occludin. After transfection with siPARD3 and siNC for 36 h, cells were fixed with 4% paraformaldehyde, ZO-1 and Occludin were observed by confocal microscope. At the same time cells were collected to detect changes in the protein levels of ZO-1 and Occludin.

cells or the polarized distribution of virus receptor. Thus, PEDV infection on the basolateral surface increased significantly.

4. Discussion

Given the importance of membrane proteins in the various cellular processes, as well as the roles they play in diseases and their potential as drug targets, it is imperative to pay more attention on them [36]. In the present work, we applied quantitative membrane proteomics to identify novel DAPs in PEDV-infected Vero cells. The proteomics approach used here was not intended to provide a comprehensive picture of all proteins changes in the PEDV-infected cells but to provide new insights into membrane proteins involved in viral infections. Among these DAPs, some proteins were found for the first time, compared with previous proteomics, such as PARD3, PTPN14, and SNX32. Although membrane proteins were extracted for identification, nuclear and cytoplasmic proteins were also identified. This could be caused by the proteins can be distributed in multiple organelles. In particular, during PEDV infection, a large number of proteins were translocated and rearranged in cells.

Studies have demonstrated that PEDV can inhibit the production of type I and III interferon and degrade CREB binding protein (CBP) [37–39]. In addition, several reports have identified many host proteins involving in the PEDV infection process, such as viperin, GTPase-activating protein-binding protein 1 (G3BP1), Mortalin and HSPB1 [40–43]. HSPB1 was also found in our results, and it was significantly down regulated (Fig. 1). By searching the relevant literature and

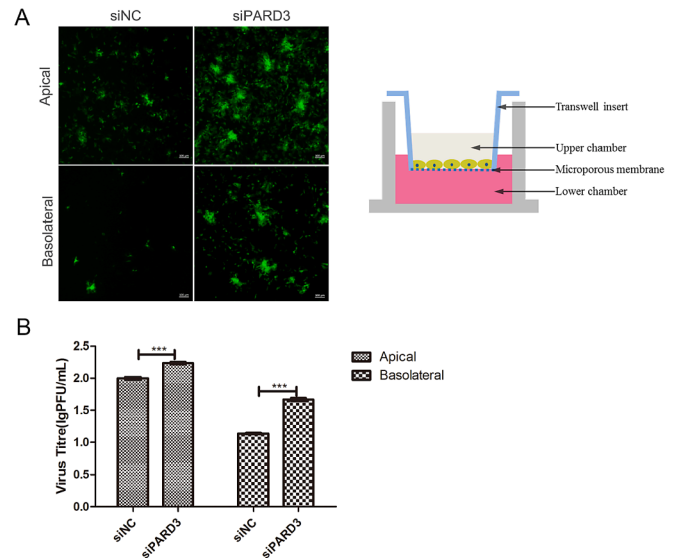


Fig. 6. Down-regulation of PARD3 promotes PEDV infection in apical and basolateral. (A) Vero cells were seeded on Transwell, when the cells were covered with 80%, siRNA-PARD3 and siNC were transfected. After 36 h, cells were infected from either apical (upper chamber) or basolateral (lower chamber) with PEDV-DR13 at MOI of 0.1. 18 h after infection, the virus were detected by immunofluorescence analysis. (B) The amount of virus infection in the apical or the basolateral was detected by plaque.

analyzing these DAPs in detail, we gained insight into the polarity related protein PARD3 which is closely related to cell tight junction. PARD3 belongs to the Post-synaptic density protein-95/Discs large/Zonula occludens-1 (PDZ) protein family, and viruses have evolved a mechanism by which they interact with their hosts, including PDZ-binding-motifs (PBMs) that interact with cellular proteins containing PDZ domains [44]. Many PDZ-containing proteins are involved in cell–cell junctions, cell polarity, recycling or trafficking [45]. Viral PBMs interact with cellular PDZs contributing to their degradation or inactivation and relocalization [44,46]. In addition to Kaposi's sarcoma associated herpesvirus (KSHV) and Human papillomavirus target PARD3 and disrupt polarity and junction formation [47,48]. PARD3 is recognized by SARS-CoV and SARS-CoV-2, but further studies are needed to decipher the functional role of PARD3 [49]. In our results, PARD3 showed a significant down-regulation at 6 h in the early stage of PEDV infection. Especially in the area of syncytial lesion caused by PEDV infection, a significant change was observed in the surrounding uninfected cells (Fig. 2C). However, PARD3 was slightly up-regulated at 12 h after virus infection compared to 6 h and 18 h (Fig. 3C), which may be caused by protein translocation or interaction with viral proteins, which needs further study. PARD3 contains three isoforms 180 kDa, 150 kDa and 100 kDa. The role of PARD3 180 kDa is to establish and maintain tight junctions in epithelial cells [50]. Here, Vero cells contained mainly PARD3 180 kDa, though there were trace amounts of PARD3 150 kDa and PARD3 100 kDa.

Studies have shown that PARD3 is predominant in the periphery of cytoplasm and cell membrane [51,52]. In uninfected Vero cells, the distribution of PARD3 was observed on the membrane through immunofluorescence, but it was difficult to observe after virus infection. At the early stage of PEDV infection, when the morphology of the membrane changed significantly, the cytoplasmic localization of PARD3 decreased significantly, and PARD3 migrated and aggregated to the nucleus in the late stage of infection under the condition of overall down-regulation (Fig. 2C). PARD3 nuclear localization seems to be associated with biologically significant events. In KSHV-positive cells PARD3 interacted with LANA led to the translocation of PARD3 from the cell periphery to a predominantly nuclear [51]. Adenoviral protein

E4orf4 can interact with PARD3 to induce nuclear rupture and tumour cell death [53]. PARD3 may act by the transfer of perinuclear actomyosin forces to modulate nuclear and cell shape changes. Interestingly, PARD3 is a large protein (180 kDa), and sequence analysis of PARD3 has putative nuclear localisation sequences. However, the occurrence of nuclear localization of PARD3 is more likely to use related nuclear localization proteins [54]. Nonetheless, the contribution of PEDV to PARD3 redistribution, the biological significance, and the mechanism of PARD3 translocation to the nucleus, remain to be elucidated and merit further investigation.

PEDV can cause protein degradation of some cellular targets [55]. In our current study, it is intriguing to find that PEDV could target PARD3 for proteasome-mediated degradation *in vitro*. Previous research has shown that Rhesus papilloma-viruses (RhpV) E7 has PBM that directs the interaction of PARD3, which it targets for proteasome-mediated degradation [56]. Viral PBM influence cell behavior through the interaction with cellular proteins containing PDZ domains, for CoVs, the PBM of E and 3a in SARS-CoV protein is the only one studied in detail and these PBMs could be involved in virus replication and pathogenesis triggering [44]. The mechanism by which PEDV degrades PARD3 is currently unknown. However, the E protein of PEDV has PBM, but it is unclear whether E mediates the change of PARD3.

Virus can destroy the key protein-protein interactions in the cell to change the protein transportation and control the cell homeostasis. Importantly, tight junctions are known to be targeted by multiple pathogenic viruses [57]. For example, respiratory syncytial virus, enteroviruses, influenza viruses and the coronavirus family increase their efficiency in disseminating by disrupting TJs [58]. PARD3, partitioning-defective 6 and atypical protein kinase C constitute the evolutionarily conserved complex partitioning defective (PAR) proteins. The Par complex plays indispensable roles in cell polarity regulation processes that establish and maintain apical-basal polarity in most animal cells, control proliferation and affect cell migration [59–61]. PARD3 can interact with cell surface proteins, such as junctional adhesion molecules, nectin, phospholipids, phosphatase and tensin homolog and Rac exchange factor Tiam1, and the depletion of PARD3 disrupts tight junction assembly [29,62–64]. PARD3 is the central component of the PAR complex and is the key regulator of epithelial tight junction formation [65]. Given that PARD3 plays a very important role in the formation of TJ, we depleted endogenous PARD3 by siRNA and found loss of PARD3 not only promoted virus infection but also increased virus adsorption and internalization. It shows that PARD3 affects the early stage of virus infection. In PARD3-downregulated Vero cells, the distribution of TJs, ZO-1 and Occludin were destroyed, which indicated the tight junction of cells was destroyed. Compared with PEDV infection, the content of ZO-1 and Occludin did not change. It indicates that downregulation of PARD3 affects the morphology of TJ, but cannot cause the degradation of TJ proteins. During PEDV infection, the TJs of the cells destroyed, and the abundance decreased. This result was consistent with previous research, indicating that PEDV infection is closely related to TJs [66–68].

More importantly, PARD3 plays a vital role in the regulation of epithelial cell polarity, especially in maintenance of apical-basal polarity [69]. Cell polarity is reflected by the polarisation and division of cell membrane into apical and basolateral domains [70]. PEDV preferentially infected Vero cells on the apical surface [35]. However, PEDV infection significantly increased in the basolateral region in PARD3-downregulated Vero cells, and the apical surface increased too. The loss of PARD3 is always accompanied by the destruction of the barrier and the loss of cell polarity. Many viruses bind to receptors on the apical sides of epithelial cells. Others target basolateral receptors, which are ordinarily inaccessible due to the TJ barrier [57]. These viruses have developed mechanisms to cause TJ disassembly, typically either through the regulation of protein abundance or localization, to reach their receptors [57]. Many viruses target cell polarity regulators, creating an replication-permissive environment and avoiding immune detection,

such as Human papillomavirus (HPV), Influenza A viruses (IAV), Adenoviruses, Flaviviruses, Coronaviruses and Rabies virus [70]. The IAV NS1 protein is able to target Scribble and Dlg1 in a PDZ-dependent fashion in epithelial cells, where the targeting of Scribble induces its relocation from the cytosol to the perinuclear region, leading to the destabilization of the tight junction and the protection of infected cells from apoptosis, thus enhancing IAV replication. At the same time NS1 targeting of these PDZ proteins in antigen-presenting cells may constitute an immune evasion mechanism [71]. The SARS E protein relocalizes tight junction-associated protein PALS1 outside of the tight junction, altering polarity establishment in epithelial cells [72]. Viral targeting of PDZ proteins usually disrupts host PDZ-dependent interactions in infected cells, thus affecting cellular functions and likely enhancing viral replication and dissemination in the host or transmission to new hosts [73]. By hijacking junctional proteins and signaling mechanisms, viruses ensure their propagation through the manipulation of the cellular homeostasis, the immune system, and tissue barriers [49].

Based on these results, we conclude that, the PDZ family protein PARD3 that can be altered by PEDV infection. Although the detailed interplay between PARD3 and PEDV remains incompletely unclear. Further work is needed to conclusively answer this question. Together, these findings provide novel insights into PEDV infection and spreading, which might be valuable for understanding PEDV-related pathogenesis.

5. Conclusions

Membrane proteomics is an ingenious method for studying membrane proteins involved in viral infection. Through quantitative membrane proteomics, the PDZ family protein PARD3 that can be altered by PEDV infection was identified for the first time. During PEDV infection, PARD3 was degraded by proteasome-dependent pathway and downregulation of PARD3 can destroy the tight junction of cells and affect the apical and basolateral sides of cells to promote PEDV infection. By hijacking proteins associated to tight junctions, viruses ensure their propagation and spread through the manipulation of the cellular homeostasis and tissue barriers. We demonstrated PARD3 is a novel antiviral protein against PEDV infection. These findings will contribute to a better understanding of the role of membrane proteins in PEDV infection.

Declaration of Competing Interest

The authors report no declarations of interest.

Data availability

No

Acknowledgements

This study was supported by the National Natural Science Foundation of China (grant 3217190467) and Henan Academy of Agricultural Sciences Fundamental Research Project (2021ZC75).

Appendix A. Supplementary data

Supplementary data to this article can be found online at <https://doi.org/10.1016/j.jprot.2021.104462>.

References

- [1] Y. Wang, M. Grunewald, S. Perlman, Coronaviruses: an updated overview of their replication and pathogenesis, *Methods Mol. Biol.* (Clifton, NJ), 2203 (2020) 1–29.
- [2] C. Lee, Porcine epidemic diarrhea virus: an emerging and re-emerging epizootic swine virus, *Virol. J.* 12 (2015) 193.
- [3] Changhee Lee, Porcine epidemic diarrhea virus: an emerging and re-emerging epizootic swine virus, *Virol. J.* 13 (2016) 1–2.

- [4] E. Wood, An apparently new syndrome of porcine epidemic diarrhoea, *Vet. Record* 100 (1977) 243–244.
- [5] W. Li, F.J.M. Van Kuppeveld, Q. He, P.J.M. Rottier, B.J. Bosch, Cellular entry of the porcine epidemic diarrhoea virus, *Virus Res.* 226 (2016) 117–127.
- [6] Fang Li, Structure, function, and evolution of coronavirus spike proteins, *Annu. Rev. Virol.* 3 (2016) 1954–1964.
- [7] M. Kishimoto, K. Uemura, T. Sanaki, A. Sato, W. Hall, H. Kariwa, et al., TMPRSS11D and TMPRSS13 activate the SARS-CoV-2 spike protein, *Viruses*. 13 (2021).
- [8] S. Matsuyama, M. Ujiike, S. Morikawa, M. Tashiro, F. Taguchi, Protease-mediated enhancement of severe acute respiratory syndrome coronavirus infection, *Proc. Natl. Acad. Sci.* 102 (2005) 12543–12547.
- [9] K. Shirato, S. Matsuyama, M. Ujiike, F. Taguchi, Role of proteases in the release of porcine epidemic diarrhoea virus from infected cells, *J. Virol.* 85 (2011) 7872–7880.
- [10] K. Radtke, K. Döhner, B. Sodeik, Viral interactions with the cytoskeleton: a hitchhiker's guide to the cell, *Cell. Microbiol.* 8 (2006) 387–400.
- [11] E. Schneeberger, R. Lynch, The tight junction: a multifunctional complex, *Am. J. Physiol. Cell Physiol.* 286 (2004). C1213–28.
- [12] C. Smallcombe, D. Linfield, T. Harford, V. Bokun, A. Ivanov, G. Piedimonte, et al., Disruption of the airway epithelial barrier in a murine model of respiratory syncytial virus infection, *Am. J. Physiol. Lung Cell. Mol. Physiol.* 316 (2019). L358–L68.
- [13] K. Teoh, Y. Siu, W. Chan, M. Schlüter, C. Liu, J. Peiris, et al., The SARS coronavirus E protein interacts with PALSI and alters tight junction formation and epithelial morphogenesis, *Mol. Biol. Cell* 21 (2010) 3838–3852.
- [14] Y. Hu, J. Song, L. Liu, Y. Zhang, L. Wang, Q. Li, microRNA-4516 contributes to different functions of epithelial permeability barrier by targeting poliovirus receptor related protein 1 in enterovirus 71 and Coxsackievirus A16 infections, *Front. Cell. Infect. Microbiol.* 8 (2018) 110.
- [15] K. Short, J. Kasper, S. van der Aa, A. Andeweg, F. Zaaraoui-Boutahar, M. Goejenbier, et al., Influenza virus damages the alveolar barrier by disrupting epithelial cell tight junctions, *Eur. Respir. J.* 47 (2016) 954–966.
- [16] K. Dokladny, M. Zuhl, P. Moseley, Intestinal epithelial barrier function and tight junction proteins with heat and exercise, *J. Appl. Physiol.* 120 (2016) 692–701.
- [17] S. Zhao, J. Gao, L. Zhu, Q. Yang, Transmissible gastroenteritis virus and porcine epidemic diarrhoea virus infection induces dramatic changes in the tight junctions and microfilaments of polarized IPEC-J2 cells, *Virus Res.* 192 (2014) 34–45.
- [18] X. Luo, L. Guo, J. Zhang, Y. Xu, W. Gu, L. Feng, et al., Tight junction protein occludin is a porcine epidemic diarrhoea virus entry factor, *J. Virol.* 91 (2017) e00202–e00217.
- [19] Zeng Songlin, Zhang Huan, Ding Zhen, et al., Proteome analysis of porcine epidemic diarrhoea virus (PEDV)-infected Vero cells, *PROTEOMICS* 15 (2015) 1819–1828.
- [20] D. Sun, H. Shi, D. Guo, J. Chen, D. Shi, Q. Zhu, et al., Analysis of protein expression changes of the Vero E6 cells infected with classic PEDV strain CV777 by using quantitative proteomic technique, *J. Virol. Methods* 218 (2015) 27–39.
- [21] Z. Li, F. Chen, S. Ye, X. Guo, A.M. Memon, M. Wu, et al., Comparative proteome analysis of porcine jejunum tissues in response to a virulent strain of porcine epidemic diarrhoea virus and its attenuated strain, *Viruses* (2016) 1999–4915.
- [22] Lin Huixing, Li Bin, Chen Lei, et al., Differential protein analysis of IPEC-J2 cells infected with porcine epidemic diarrhoea virus pandemic and classical strains elucidates the pathogenesis of infection, *J. Proteome Res.* 16 (2017) 2113–2120.
- [23] Y. Su, Y. Liu, Y. Chen, G. Xing, H. Hao, Q. Wei, et al., A novel duplex TaqMan probe-based real-time RT-qPCR for detecting and differentiating classical and variant porcine epidemic diarrhoea viruses, *Mol. Cell. Probes* 37 (2018) 6–11.
- [24] Ma Jie, Chen Tao, Wu Songfeng, et al., iProX: an integrated proteome resource, *Nucleic Acids Res.* 47 (2018) D1211–D1217.
- [25] Y. Wang, W. Le, Autophagy and ubiquitin-proteasome system, *Adv. Exp. Med. Biol.* 1206 (2019) 527–550.
- [26] P. Grumati, I. Dikic, Ubiquitin signaling and autophagy, *J. Biol. Chem.* 293 (2018) 5404–5413.
- [27] Y.T. Wu, H.L. Tan, G. Shui, C. Bauvy, H.M. Shen, Dual role of 3-methyladenine in modulation of autophagy via different temporal patterns of inhibition on class I and III phosphoinositide 3-kinase, *J. Biol. Chem.* 285 (2010) 10850–10861.
- [28] G. Lin, G. Joberty, I.G. Macara, Assembly of epithelial tight junctions is negatively regulated by Par6, *Curr. Biol.* 12 (2002) 221–225.
- [29] K. Ebnat, A. Suzuki, Y. Horikoshi, T. Hirose, Meyer Zu, M. Brickwedde, S. Ohno, et al., The cell polarity protein ASIP/Par-3 directly associates with junctional adhesion molecule (JAM), *EMBO J.* 20 (2001) 3738–3748.
- [30] B. Goldstein, I. Macara, The PAR proteins: fundamental players in animal cell polarization, *Dev. Cell* 13 (2007) 609–622.
- [31] J. Rossen, C. Bekker, W. Voorhout, G. Strous, A. van der Ende, P. Rottier, Entry and release of transmissible gastroenteritis coronavirus are restricted to apical surfaces of polarized epithelial cells, *J. Virol.* 68 (1994) 7966–7973.
- [32] C.T.K. Tseng, J. Tseng, L. Perrone, M. Worthy, V. Popov, C.J. Peters, Apical entry and release of severe acute respiratory syndrome-associated coronavirus in polarized Calu-3 lung epithelial cells, *J. Virol.* 79 (2005) 9470–9479.
- [33] A. Vanderheiden, P. Ralfs, T. Chirkova, A. Upadhyay, M. Zimmerman, S. Bedoya, et al., Type I and type III interferons restrict SARS-CoV-2 infection of human airway epithelial cultures, *J. Virol.* 94 (2020) e00985–20.
- [34] G. Wang, C. Deering, M. Macke, J. Shao, R. Burns, D. Blau, et al., Human coronavirus 229E infects polarized airway epithelia from the apical surface, *J. Virol.* 74 (2000) 9234–9239.
- [35] Y. Cong, X. Li, Y. Bai, X. Lv, G. Herrler, L. Enjuanes, et al., Porcine aminopeptidase N mediated polarized infection by porcine epidemic diarrhoea virus in target cells, *Virology*. 478 (2015) 1–8.
- [36] S. Tan, H. Tan, M. Chung, Membrane proteins and membrane proteomics, *Proteomics*. 8 (2008) 3924–3932.
- [37] Q. Zhang, K. Shi, D. Yoo, Suppression of type I interferon production by porcine epidemic diarrhoea virus and degradation of CREB-binding protein by nsp1, *Virology*. 489 (2016) 252–268.
- [38] L. Cao, X. Ge, Y. Gao, G. Herrler, Y. Ren, X. Ren, et al., Porcine epidemic diarrhoea virus inhibits dsRNA-induced interferon- β production in porcine intestinal epithelial cells by blockade of the RIG-I-mediated pathway, *Virol. J.* 12 (2015) 127.
- [39] Q. Zhang, H. Ke, A. Blikslager, T. Fujita, D. Yoo, Type III interferon restriction by porcine epidemic diarrhoea virus and the role of viral protein nsp1 in IRF1 signaling, *J. Virol.* 92 (2018) e01677–17.
- [40] M. Sun, Z. Yu, J. Ma, Z. Pan, C. Lu, H. Yao, Down-regulating heat shock protein 27 is involved in porcine epidemic diarrhoea virus escaping from host antiviral mechanism, *Vet. Microbiol.* 205 (2017) 6–13.
- [41] B. Fan, L. Zhu, X. Chang, J. Zhou, R. Guo, Y. Zhao, et al., Mortalin restricts porcine epidemic diarrhoea virus entry by downregulating clathrin-mediated endocytosis, *Vet. Microbiol.* 239 (2019), 108455.
- [42] K. Pandey, S. Zhong, D. Diel, Y. Hou, Q. Wang, E. Nelson, et al., GTPase-activating protein-binding protein 1 (G3BP1) plays an antiviral role against porcine epidemic diarrhoea virus, *Vet. Microbiol.* 236 (2019), 108392.
- [43] J. Wu, H. Chi, Y. Fu, A. Cao, J. Shi, M. Zhu, et al., The antiviral protein viperin interacts with the viral N protein to inhibit proliferation of porcine epidemic diarrhoea virus, *Arch. Virol.* 165 (2020) 2279–2289.
- [44] C. Castaño-Rodríguez, J. Honrubia, J. Gutiérrez-Álvarez, I. Sola, L. Enjuanes, Viral PDZ binding motifs influence cell behavior through the interaction with cellular proteins containing PDZ domains, *Methods Mol. Biol. (Clifton, NJ)*. 2256 (2021) 217–236.
- [45] C. James, S. Roberts, Viral Interactions with PDZ Domain-Containing Proteins-An Oncogenic Trait? *Pathogens* (Basel, Switzerland), 2016, p. 5.
- [46] E. Terrien, A. Chaffotte, M. Lafage, Z. Khan, C. Préhaud, F. Cordier, et al., Interference with the PTEN-MAST2 interaction by a viral protein leads to cellular relocalization of PTEN, *Sci. Signal.* 5 (2012) ra58.
- [47] F. Facciuto, M. Bugnon Valdano, F. Marziali, P. Massimi, L. Banks, A.L. Cavatorta, et al., Human papillomavirus (HPV)-18 E6 oncoprotein interferes with the epithelial cell polarity Par3 protein, *Mol. Oncol.* 8 (2014) 533–543.
- [48] Y. Yoshimatsu, T. Nakahara, K. Tanaka, Y. Inagawa, M. Narisawa-Saito, T. Yugawa, et al., Roles of the PDZ-binding motif of HPV 16 E6 protein in oncogenic transformation of human cervical keratinocytes, *Cancer Sci.* 108 (2017) 1303–1309.
- [49] C. Caillet-Saguy, F. Durbesson, V. Rezelj, G. Gogl, Q. Tran, J. Twizere, et al., Host PDZ-containing proteins targeted by SARS-CoV-2, *FEBS J.* 288 (2021) 5148–5162.
- [50] Z. Ying, F. Longhou, D. Dan, Z. Wenchoa, F. Xiujing, C. Jiwu, et al., Proteome identification of binding-partners interacting with cell polarity protein Par3 in Jurkat cells, *Acta Biochim. Biophys. Sin.* 40 (2008) 729–739.
- [51] H. Jha, Z. Sun, S. Upadhyay, D. El-Naccache, R. Singh, S. Sahu, et al., KSHV-mediated regulation of Par3 and SNAIL contributes to B-cell proliferation, *PLoS Pathog.* 12 (2016), e1005801.
- [52] K. Ebnat, M. Aurrand-Lions, A. Kuhn, F. Kiefer, S. Butz, K. Zander, et al., The junctional adhesion molecule (JAM) family members JAM-2 and JAM-3 associate with the cell polarity protein PAR-3: a possible role for JAMs in endothelial cell polarity, *J. Cell Sci.* 116 (2003) 3879–3891.
- [53] C. Dzienelewski, M. Rodrigue, A. Caillier, K. Jacquet, M. Boulanger, J. Bergeman, et al., Adenoviral protein E4orf4 interacts with the polarity protein Par3 to induce nuclear rupture and tumor cell death, *J. Cell Biol.* 219 (2020) e201805122.
- [54] L. Fang, Y.G. Wang, D. Du, G. Yang, T.T. Kwok, S.K. Kong, et al., Cell polarity protein Par3 complexes with DNA-PK and regulates DNA double-strand break repair, *Cell Res.* 17 (2007) 572–574.
- [55] L. Guo, X. Luo, R. Li, Y. Xu, J. Zhang, J. Ge, et al., Porcine epidemic diarrhoea virus infection inhibits interferon signaling by targeted degradation of STAT1, *J. Virol.* 90 (2016) 8281–8292.
- [56] V. Tomaić, D. Gardiol, P. Massimi, M. Ozbun, M. Myers, L. Banks, Human and primate tumour viruses use PDZ binding as an evolutionarily conserved mechanism of targeting cell polarity regulators, *Oncogene*. 28 (2009) 1–8.
- [57] J. Torres-Flores, C. Arias, Tight junctions go viral!, *Viruses*. 7 (2015) 5145–5154.
- [58] D. Linfield, A. Raduka, M. Aghapour, F. Rezaee, Airway tight junctions as targets of viral infections, *Tissue Barriers* 9 (2021) 1883965.
- [59] T. Nishimura, K. Kaibuchi, Numb controls integrin endocytosis for directional cell migration with aPKC and PAR-3, *Dev. Cell* 13 (2007) 15–28.
- [60] D. Rivers, S. Moreno, M. Abraham, J. Ahringer, PAR proteins direct asymmetry of the cell cycle regulators polo-like kinase and Cdc25, *J. Cell Biol.* 180 (2008) 877–885.
- [61] E. Rodriguez-Boulan, I. Macara, Organization and execution of the epithelial polarity programme, *Nat. Rev. Mol. Cell Biol.* 15 (2014) 225–242.
- [62] Xinyu Chen, Ian Macara, G., Par-3 controls tight junction assembly through the Rac exchange factor Tiam1, *Nat. Cell Biol.* 7 (2005) 262–269.
- [63] W. Feng, H. Wu, L.N. Chan, M. Zhang, Par-3-mediated junctional localization of the lipid phosphatase PTEN is required for cell polarity establishment, *J. Biol. Chem.* 283 (2008) 23440–23449.
- [64] K. Takekuni, W. Ikeda, T. Fujito, K. Morimoto, M. Takeuchi, M. Monden, et al., Direct binding of cell polarity protein PAR-3 to cell-cell adhesion molecule nectin at neuroepithelial cells of developing mouse, *J. Biol. Chem.* 278 (2003) 5497–5500.
- [65] I. Chuykin, O. Ossipova, S. Sokol, Par3 interacts with Prickle3 to generate apical PCP complexes in the vertebrate neural plate, *eLife*. 7 (2018) e37881.

- [66] Y. Chen, E. Helm, J. Groeltz-Thrush, N. Gabler, E. Burrough, Epithelial-mesenchymal transition of absorptive enterocytes and depletion of Peyer's patch M cells after PEDV infection, *Virology*. 552 (2021) 43–51.
- [67] K. Jung, B. Eyerly, T. Annamalai, Z. Lu, L. Saif, Structural alteration of tight and adherens junctions in villous and crypt epithelium of the small and large intestine of conventional nursing piglets infected with porcine epidemic diarrhea virus, *Vet. Microbiol.* 177 (2015) 373–378.
- [68] Q. Zong, Y. Huang, L. Wu, Z. Wu, S. Wu, W. Bao, Effects of porcine epidemic diarrhea virus infection on tight junction protein gene expression and morphology of the intestinal mucosa in pigs, *Pol. J. Vet. Sci.* 22 (2019) 345–353.
- [69] C. Royer, X. Lu, Epithelial cell polarity: a major gatekeeper against cancer? *Cell Death Differ.* 18 (2011) 1470–1477.
- [70] M. Thomas, L. Banks, Upsetting the balance: when viruses manipulate cell polarity control, *J. Mol. Biol.* 430 (2018) 3481–3503.
- [71] L. Golebiewski, H. Liu, R. Javier, A. Rice, The avian influenza virus NS1 ESEV PDZ binding motif associates with Dlg1 and scribble to disrupt cellular tight junctions, *J. Virol.* 85 (2011) 10639–10648.
- [72] M. DeDiego, J. Nieto-Torres, J. Jimenez-Guardaño, J. Regla-Nava, C. Castaño-Rodríguez, R. Fernandez-Delgado, et al., Coronavirus virulence genes with main focus on SARS-CoV envelope gene, *Virus Res.* 194 (2014) 124–137.
- [73] R. Javier, A. Rice, Emerging theme: cellular PDZ proteins as common targets of pathogenic viruses, *J. Virol.* 85 (2011) 11544–11556.